

Strong terahertz radiation from relativistic laser interaction with solid density plasmas

Y. T. Li, C. Li, M. L. Zhou, W. M. Wang, F. Du, W. J. Ding, X. X. Lin, F. Liu, Z. M. Sheng, X. Y. Peng, L. M. Chen, J. L. Ma, X. Lu, Z. H. Wang, Z. Y. Wei, and J. Zhang

Citation: [Applied Physics Letters](#) **100**, 254101 (2012); doi: 10.1063/1.4729874

View online: <http://dx.doi.org/10.1063/1.4729874>

View Table of Contents: <http://scitation.aip.org/content/aip/journal/apl/100/25?ver=pdfcov>

Published by the [AIP Publishing](#)

Articles you may be interested in

[Intense terahertz emission from relativistic circularly polarized laser pulses interaction with overdense plasmas](#)
Phys. Plasmas **20**, 103115 (2013); 10.1063/1.4826508

[A study of fast electron energy transport in relativistically intense laser-plasma interactions with large density scalelengths](#)
Phys. Plasmas **19**, 053104 (2012); 10.1063/1.4714615

[Relativistic effects in the interaction of high intensity ultra-short laser pulse with collisional underdense plasma](#)
Phys. Plasmas **18**, 093108 (2011); 10.1063/1.3633529

[Relativistic second harmonic generation from an S-polarized laser in over-dense plasma](#)
Phys. Plasmas **18**, 083105 (2011); 10.1063/1.3624496

[Generation of highly collimated high-current ion beams by skin-layer laser-plasma interaction at relativistic laser intensities](#)
Appl. Phys. Lett. **89**, 061504 (2006); 10.1063/1.2266232

The logo for AIP Chaos is displayed on a red background with a geometric, low-poly pattern. The letters 'AIP' are in a large, white, sans-serif font, followed by a vertical bar and the word 'Chaos' in a smaller, white, sans-serif font.

AIP | Chaos

CALL FOR APPLICANTS
Seeking new Editor-in-Chief

Strong terahertz radiation from relativistic laser interaction with solid density plasmas

Y. T. Li (李玉同),^{1,a)} C. Li (李春),¹ M. L. Zhou (周木林),¹ W. M. Wang (王伟民),¹ F. Du (杜飞),¹ W. J. Ding (丁文君),¹ X. X. Lin (林晓宣),¹ F. Liu (刘峰),¹ Z. M. Sheng (盛政明),^{1,2} X. Y. Peng (彭晓昱),³ L. M. Chen (陈黎明),¹ J. L. Ma (马景龙),¹ X. Lu (鲁欣),¹ Z. H. Wang (王兆华),¹ Z. Y. Wei (魏志义),¹ and J. Zhang (张杰)^{1,2,a)}

¹Beijing National Laboratory for Condensed Matter Physics, Institute of Physics, Chinese Academy of Sciences, Beijing 100190, China

²Key Laboratory for Laser Plasmas (MoE) and Department of Physics, Shanghai Jiao Tong University, Shanghai 200240, China

³Institute of Materials Research and Engineering, A*STAR, 3 Research Link, Singapore 117602, Singapore

(Received 3 February 2012; accepted 4 June 2012; published online 19 June 2012)

We report a plasma-based strong THz source generated in intense laser-solid interactions at relativistic intensities $>10^{18}$ W/cm². Energies up to 50 μ J/sr per THz pulse is observed when the laser pulses are incident onto a copper foil at 67.5°. The temporal properties of the THz radiation are measured by a single shot, electro-optic sampling method with a chirped laser pulse. The THz radiation is attributed to the self-organized transient fast electron currents formed along the target surface. Such a source allows potential applications in THz nonlinear physics and provides a diagnostic of transient currents generated in intense laser-solid interactions. © 2012 American Institute of Physics. [<http://dx.doi.org/10.1063/1.4729874>]

Terahertz (THz) radiation, which is located between the infrared light and microwaves in the frequency domain, attracts much interest due to its wide applications.¹ Tabletop THz sources can be generated by using optical pulses to pump various neutral materials.²⁻⁵ With the tilted laser wavefront scheme,⁶⁻⁸ THz pulse energies up to 30 μ J has been obtained. On the other hand, plasma is a promising medium to generate strong THz radiation,⁹ which overcomes the damage problem of neutral materials when the pump laser intensity is high. Observations of THz radiation from femtosecond laser-induced plasma filaments in air or in other low density gases have been reported.^{10,11} By applying a “bias field,” which is provided by an external electric field or a “second harmonic optical field,” such THz radiation can be much enhanced.¹²⁻¹⁷ However, the radiation is subject to saturation due to the limitation of laser intensity (typical $<10^{15}$ W/cm², resulting from plasma defocusing effect¹⁸), low electron number, and THz re-absorption.^{16,19}

In contrast to neutral materials and plasma filaments in low density gases, almost arbitrarily high laser energies and intensities can be used in laser-solid interactions. THz pulses with energies of 1 μ J/sr were observed from solid targets irradiated by laser pulses at optical intensities $\sim 10^{19}$ W/cm².²⁰ Sagisaka *et al.* also obtained 0.5 μ J/sr THz pulses from thin foil targets.²¹ These observations show the feasibility to produce strong THz sources with solid targets irradiated by high intensity laser pulses, though the generation mechanisms are still not well understood.²² Obviously, the THz emission in such interactions shall be relevant with the generation of fast electron beams. It has been reported that the ultrafast electron bunches produced from laser wakefield acceleration in underdense plasma can result in powerful THz emission with

energy about 3–5 μ J/sr per pulse at the plasma-vacuum boundary via transition radiation.^{23,24} Since the electron bunches produced in laser-solid interaction may contain more charges, in principle, one can expect more powerful THz emission.

In this Letter, we present experimental and theoretical investigations on THz pulse generation in the relativistic laser-solid interactions. Strong THz emission with energy ~ 50 μ J/sr per pulse is observed. The polarization, temporal, and spectral properties of the THz pulse are characterized. It is believed that a transient self-organized fast electron current along the target surface is mainly responsible for the observed THz pulse generation.

The experiments were carried out using the xtreme light II (XL-II) Ti: sapphire laser system at the Institute of Physics, Chinese Academy of Sciences. Figure 1 shows a schematic view of the THz measurement. A linearly polarized laser pulse with an energy up to 150 mJ in 100 fs at 800 nm was focused onto a 30 μ m thick copper foil at an incidence angle 67.5° using an

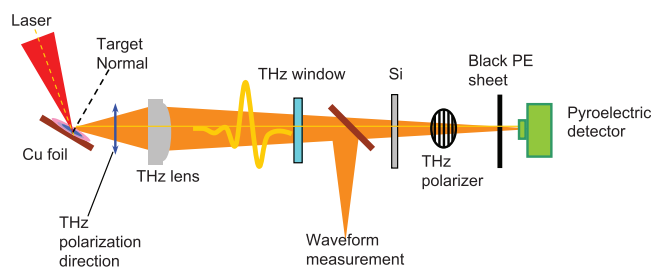


FIG. 1. Schematic of the THz measurements. A femtosecond laser pulse was focused onto a copper foil at 67.5° in the vacuum chamber. A THz lens aligned in the specular direction was used to collect the THz emission. After the THz vacuum transmission window, the collected THz pulse was split by a pellicle into two arms. The transmitted one went into a pyroelectric detector for energy measurement. The reflected one for waveform measurement. The polarization of the THz pulse was measured by a wire-grid polarizer.

^{a)}Author to whom correspondence should be addressed. Electronic mail: ytli@aphy.iphy.ac.cn or jzhang1@sju.edu.cn.

$f/3.5$ off-axis parabolic mirror. The laser pulse can be p - or s -polarized by using a half wave plate. The target size was $100 \times 200 \text{ mm}^2$. The diameter of the focal spot was $\sim 5 \mu\text{m}$. The corresponding laser intensity was up to $2.7 \times 10^{18} \text{ W/cm}^2$. A THz lens with a collection solid angle 0.11 sr , aligned in the specular direction, was used to collect the THz emission. After a THz vacuum transmission window, the collected THz pulse was split by a pellicle into two arms. The transmitted one went into a calibrated pyroelectric detector with a response range from 0.3 to 21 THz for energy measurement, while the reflected one for temporal waveform measurement. Silicon and plastic filters were set before the pyroelectric detector to transmit the THz radiation and block the visible light. The polarization of the THz pulse was measured by a wire-grid polarizer.

The waveform was measured by electro-optic sampling method with a chirped laser pulse.^{25,26} In our solid experiment, we fired the laser in every few minutes. To obtain the waveform in a real single shot, we have developed a modified spectral-encoding detection system, in which the chirped probe beam was split into two parts, the reference beam and the beam modulated by the THz pulses. The two beams were sent to the same imaging spectrometer with two fibers simultaneously. In this way, we could obtain the spectra of the reference and modulated beam simultaneously.

Figure 2 shows the measured waveform and the normalized spectrum of the THz radiation produced when a p -polarized laser pulse is incident onto the target surface. The whole width of the THz pulse is about 1.5 ps . The peak frequency is about 0.5 THz . Note that there is a high frequency detection cutoff for a ZnTe crystal due to the first transverse optical phonon resonance.²⁷ After considering the dispersion effect, the cutoff is about 2.5 THz for the 1 mm thick ZnTe used in our experiment.²⁸ To overcome the limitation of the spectral encoding system, a set of low-pass multi-mesh filters with edges at $10, 5, 3, 1 \text{ THz}$ were also used in front of the pyroelectric detector to estimate the spectrum. It is found that most THz energies are concentrated below 1 THz even though the whole emission is extended to a wide range up to 20 THz . Considering the lower limit of the detector, the result obtained with the filter method indicates that the peak of the THz emission spectrum is between 0.3 – 1 THz . This agrees with the result given by the spectral encoding method.

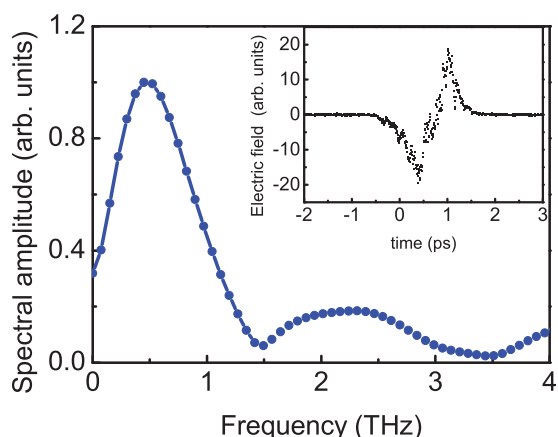


FIG. 2. Normalized spectrum of the THz radiation. The inset is the temporal waveform measured by a single-shot electric-optic sampling method.

There are two main distortions often observed in THz measurement with the spectral encoding technique.^{26,29–31} The first comes from the mismatch between the detection time window or the chirp rate of the probe pulse and THz pulse length, the second stems from the strong THz signal due to the omit of the quadratic part of the modulation strength. Since the result obtained by the spectral encoding method is consistent with that by the filter method, as well as the normalized intensity of the lower frequency part of the THz spectrum is relatively low (only 0.4 at the beginning), these two distortions in our measurements should be small.

Figure 3 shows the dependence of the THz pulse energy on pump laser energy. Each data point was taken by an average of ~ 10 shots. The energy of the THz radiation monotonically increases with laser energy. For the laser energy of 130 mJ , the THz energy is up to $5.5 \mu\text{J}$ in 0.11 sr , which corresponds to $50 \mu\text{J/sr}$. We find that the radiation is dependent on the preplasma density scale length.³² Unlike laser-gas interactions,¹⁶ no saturation effect is observed.

In our previous experiments, we also measured the angular distribution of THz radiation.³³ The results show that the THz pulse is not collimated but emitted into the space in front of the target with a very large divergence angle. With the measured energy and angular distribution of the THz pulse, the total conversion efficiency from laser energy to THz pulse is estimated to be $>10^{-3}$, which is similar to the two-color field¹⁶ and titled wavefront⁶ schemes. Higher THz pulse energy could be achieved if the laser energy or intensity is further increased.

Figure 4 shows the THz intensity as a function of the rotation angle of the wire-grid polarizer for p - and s -polarized laser pulses, respectively. We find that the THz polarization direction is always within the laser incident plane (which is defined by the laser propagation axis and the target normal), no matter the incident laser pulse is p - or s -polarized. The THz polarization direction is illustrated by a blue arrow in Fig. 1. The polarization extinction ratio is about $10:1$. The maximum THz intensity for the s -polarized laser pulse is lower by ~ 5 times than that for the p -polarized. The fact that the radiation is polarized indicates that the measured signals are not thermal emission.

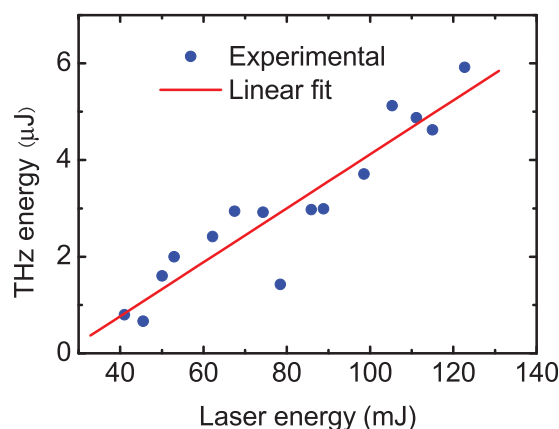


FIG. 3. THz pulse energy as a function of the pump laser energy when the laser pulse is p -polarized. The THz pulse energy increases with the laser energy, which reaches $5.5 \mu\text{J}$ in a solid angle 0.11 sr for the pump laser energy of 130 mJ .

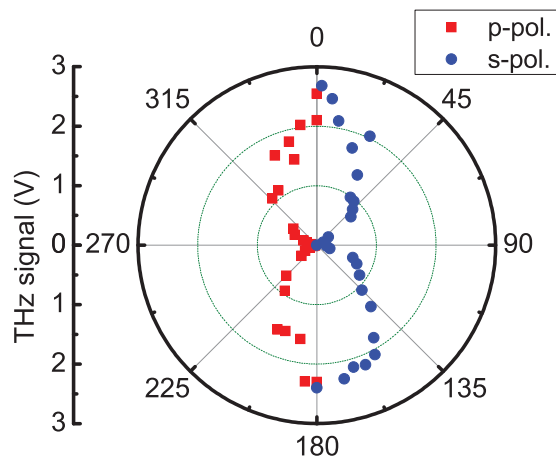


FIG. 4. THz polarization measurement by detecting the THz intensity as a function of the rotation angle of the polarizer for the *s*-polarized (blue circle, 0° – 180°) and *p*-polarized (red square, 180° – 360°) laser pulses. The data for the *s*-polarized laser pulses are artificially multiplied by a factor of 5 for clear comparison.

Two generation mechanisms have been proposed for the THz radiation in the laser-solid interactions, accelerated current arising from the longitudinal ponderomotive force²⁰ and “antenna mechanism.”²¹ The two mechanisms are not sufficient to explain the features we have observed. If the current is driven by the longitudinal ponderomotive force, the current and the THz radiation will be almost independent of the incident laser polarization. This, however, is different from our experimental observation that a 5-time enhancement in the THz output energy for *p*-polarized laser pulses comparing with that for the *s*-polarized light. According to “antenna” model, in which the THz frequency is determined by the target size, our 100×200 mm Cu foil targets will generate THz radiation at ~ 0.006 THz. This is much different from our measurement. When the laser pulse is focused on the target at different distances from the target edge, the THz frequency did not change either. Gao *et al.* also did not observe clear correlation between the THz frequency and the target size when a long wire was used as a target.²²

The strong THz radiation observed indicates that a net current should be excited in the plasma. In the interaction of a relativistic laser pulse with a solid foil, energetic (fast) electrons with a temperature from several hundreds keV to several MeV can be generated.^{34,35} These fast electrons will form a transient current. There are two kinds of currents that can be formed in the interaction. One is a longitudinal current generated by the ponderomotive force of the relativistic laser pulse in the laser propagation direction. This kind current basically exists in the high density region. The observed THz radiation in our experiments should not be induced by the longitudinal current, since the THz wave cannot escape from the high density region. Another is the lateral current, which comes from the fast electrons propagating nearly along the target surface due to the confinement of the spontaneous quasistatic magnetic and electrostatic fields at the surface.^{36–39} The lateral current will be strong when the laser incidence angle is large. In our experiments, we find that the dependence of the THz radiation on laser conditions (polarization, intensity, etc.) is quite similar to that of the lateral current. This enables us to believe that the THz radiation

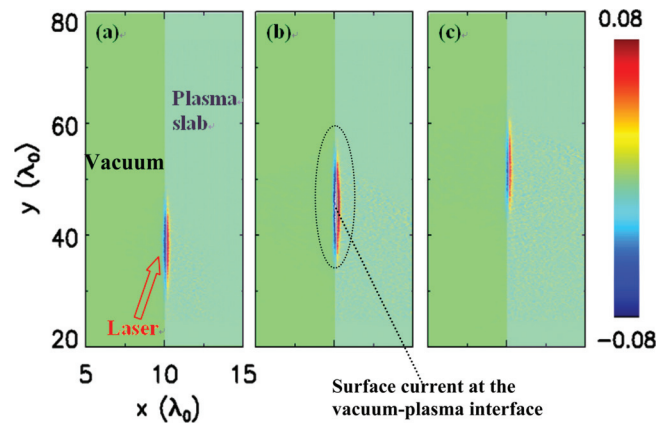


FIG. 5. Electron current distributions at the target surface obtained from 2D PIC simulations. The whole simulation space consists of two regions, a vacuum (green) and target plasma (gray) region. An 80 fs *p*-polarized laser pulse is incident from the vacuum onto the plasma surface at 60° with an intensity of 2.6×10^{18} W/cm². The front target surface is located at $x = 10 \lambda_0$. The electron current distributions at the time of 50 (a), 60 (b), and 70 (c) laser cycles are shown. One can see that a clear current sheet is excited along the vertical vacuum-plasma interface. The current flows in the *y*-direction with time.

observed may originate from the lateral current. To check this, we have performed two-dimensional (2D) particle-in-cell (PIC) simulations to observe the surface current distributions under our experimental conditions.

In the simulations, the target is an overdense plasma slab located in the region 10 – $15 \lambda_0$ in *x*-direction and 20 – $80 \lambda_0$ in *y*-direction, where λ_0 is the laser wavelength (see Fig. 5). The target density is $6n_c$, where n_c is the critical density. A *p*-polarized laser pulse is launched at the position $(0,0)$ and irradiate on the front target surface at an incidence angle 60° with an intensity 2.6×10^{18} W/cm². The laser pulse duration is 80 fs and the size of the laser focal spot is $6 \mu\text{m}$. In the simulations, the spatial cell size is 0.05 laser wavelength, the temporal resolution is 0.025 laser cycle, and there are 25 electrons and ions per cell. Figure 5 shows the simulated distributions of the electron current along the *y*-direction at the time of 50, 60, and 70 laser cycles after the laser pulse is launched. We can see that a well-confined electron current sheet is excited along the vertical vacuum-target interface. The depth of the current sheet in the *x*-direction is far less than λ_0 . The current flows in the *y*-direction with time.

A picosecond-order timescale (for example, a THz wave at 0.1 THz corresponds to a timescale 10 ps) is required to observe the complete process of the THz wave generation. This is extremely difficult for PIC simulations, since serious numerical noise will arise for high density solid plasmas in several picoseconds. In our experiment, the sizes of the laser focus and the surface current are much smaller than both the distance from the plasma to the detector, R_0 , and $\sqrt{2R_0\lambda_T}$, where λ_T is the wavelength of the THz radiation. Therefore, we can consider the current as a point source and ignore the phase differences of the radiation at different positions of the current.⁴⁰ Thus, we can use a far field approximation model to describe the features of the THz pulses originated from the lateral current qualitatively. Since simulations and observations show that the surface current strength is increased with the laser intensity, I_0 , the surface current can be expressed as $\vec{J} \sim J_0 \exp(-t^2/\tau_0^2) \delta(\vec{r}) \vec{e}_y$, where $1.665\tau_0$ is the full width at half maximum of the laser duration, J_0 is the

peak current, which is in proportion to I_0 . According to the far field approximation, the THz electric field at the detector is written as $\vec{E}_{THz} \sim \frac{2J_0 \exp(-t^2/\tau_0^2)}{c^2 \tau_0^3 R_0 (1 + \vec{n} \cdot \vec{\beta})} \vec{n} \times (\vec{n} \times \vec{e}_y)$, where \vec{n} is the unit vector directing from the current center to the detector, $\vec{\beta}$ is the average velocity of the electrons in the current, and c is the speed of light.

With surface current source and the model, we can understand most features of the observed THz radiation. From the expression of \vec{E}_{THz} , we can see the THz amplitude increasing with the laser intensity, like the results in Fig. 3. The model indicates that the THz radiation in the laser incident plane is always p -polarization, no matter a p - or s -polarized pump laser pulse is used. This is in agreement with the result in Fig. 4, in which the data are measured by the detector set in the incident plane. More laser energy is deposited into the plasma with a p -polarized laser pulse than with an s -polarized laser pulse.⁴¹ This will lead to a stronger current and a consequent stronger THz radiation for the p -polarized laser pulse. The radiation energy per solid angle of the THz source can be expressed as $dP_\Omega/d\Omega \sim \int_{-\infty}^{+\infty} \left| \frac{\vec{n}c}{4\pi} \vec{E}_{THz} \right|^2 dt$

$R_0^2 dt = \frac{J_0^2 \sin^2 \theta}{16\sqrt{\pi}c^3 \tau_0 (1 + \beta \cos \theta)^3}$, where θ is the angle between \vec{n} and $\vec{\beta}$. The angular distribution obtained from this equation is also consistent with that measured in our experiment.³³

Using the measured THz radiation and the approximate model, we can estimate the magnitude of the transient current generated in the intense laser-solid interactions. Taking $dP_\Omega/d\Omega \sim 50 \mu\text{J}/\text{sr}$ and $\beta \sim 0.78c$ (corresponding to a fast electron temperature 300 keV),³⁶ the peak magnitude of the current is ~ 10 MA, which indicates $\sim 10^{12}$ electrons generated during the laser duration.

In summary, a strong tabletop THz source from femto-second laser-solid interactions has been generated at the relativistic laser intensity $> 10^{18} \text{W}/\text{cm}^2$. The energy of a single THz pulse can be up to $50 \mu\text{J}/\text{sr}$ with only ~ 100 mJ laser pulses. The total conversion efficiency from the laser pulse to the THz radiation in the whole space is $> 10^{-3}$. A self-organized fast electron current model is proposed to understand the generation of THz radiation. More powerful THz pulses with energies up to mJ or even higher are expected with petawatt laser systems available nowadays. Such sources would allow some applications in the THz range, such as real time imaging of dynamical process of materials with picosecond time resolution, excitation of non-linear phenomena, etc. Furthermore, the THz radiation is also a diagnostic of the transient electron currents generated during relativistic laser-plasma interactions.

We thank S. C. Shi and C. L. Zhang for calibrating the detectors and filters and L. Wang for discussions. This work is supported by the National Nature Science Foundation of China (Grant Nos. 10925421, 11135012, 11105217, and 11121504).

¹M. Tonouchi, *Nat. Photonics* **1**, 97 (2007).

²A. S. Weling, B. B. Hu, N. M. Froberg, and D. H. Auston, *Appl. Phys. Lett.* **64**, 137 (1994).

³X. C. Zhang, B. B. Hu, N. M. Froberg, and D. H. Auston, *Appl. Phys. Lett.* **56**, 1011 (1990).

- ⁴R. Kersting, K. Unterrainer, G. Strasser, H. F. Kauffmann, and E. Gornik, *Phys. Rev. Lett.* **79**, 3038 (1997).
- ⁵F. Kadlec, P. Kužel, and J. L. Coutaz, *Opt. Lett.* **29**, 2674 (2004).
- ⁶A. G. Stepanov, L. Bonacina, S. V. Chekalin, and J. P. Wolf, *Opt. Lett.* **33**, 2497 (2008).
- ⁷L. Pálfalvi, J. A. Fülöp, G. Almási, and J. Hebling, *Appl. Phys. Lett.* **92**, 171107 (2008).
- ⁸K.-L. Yeh, M. C. Hoffmann, J. Hebling, and K. A. Nelson, *Appl. Phys. Lett.* **90**, 171121 (2007).
- ⁹Z. M. Sheng, K. Mima, J. Zhang, and H. Sanuki, *Phys. Rev. Lett.* **94**, 095003 (2005).
- ¹⁰C. D'Amico, A. Houard, M. Franco, B. Prade, A. Mysyrowicz, A. Couairon, and V. T. Tikhonchuk, *Phys. Rev. Lett.* **98**, 235002 (2007).
- ¹¹Y. Liu, A. Houard, B. Prade, S. Akturk, A. Mysyrowicz, and V. T. Tikhonchuk, *Phys. Rev. Lett.* **99**, 135002 (2007).
- ¹²A. Houard, Y. Liu, B. Prade, V. T. Tikhonchuk, and A. Mysyrowicz, *Phys. Rev. Lett.* **100**, 255006 (2008).
- ¹³D. J. Cook and R. M. Hochstrasser, *Opt. Lett.* **25**, 1210 (2000).
- ¹⁴D. You, R. R. Jones, P. H. Bucksbaum, and D. R. Dykaar, *Opt. Lett.* **18**, 290 (1993).
- ¹⁵X. Xie, J. Dai, and X. C. Zhang, *Phys. Rev. Lett.* **96**, 075005 (2006).
- ¹⁶K. Y. Kim, A. J. Taylor, J. H. Glowina, and G. Rodriguez, *Nat. Photonics* **2**, 605 (2008).
- ¹⁷T. Bartel, P. Gaal, K. Reimann, M. Woerner, and T. Elsaesser, *Opt. Lett.* **30**, 2805 (2005).
- ¹⁸A. Couairon and A. Mysyrowicz, *Phys. Rep.* **441**, 47 (2007).
- ¹⁹W. M. Wang, Z. M. Sheng, H. C. Wu, M. Chen, C. Li, J. Zhang, and K. Mima, *Opt. Express* **16**, 16999 (2008).
- ²⁰H. Hamster, A. Sullivan, S. Gordon, W. White, and R. W. Falcone, *Phys. Rev. Lett.* **71**, 2725 (1993).
- ²¹A. Sagiska, H. Daido, S. Nashima, S. Orimo, K. Ogura, M. Mori, A. Yogo, J. Ma, I. Daito, A. S. Pirozhkov, S. V. Bulanov, T. Zh. Esirhepov, K. Shimizu, and M. Hosoda, *Appl. Phys. B* **90**, 373 (2008).
- ²²Y. Gao, T. Drake, Z. Chen, and M. F. DeCamp, *Opt. Lett.* **33**, 2776 (2008).
- ²³W. P. Leemans, C. G. R. Geddes, J. Faure, Cs. Tóth, J. van Tilborg, C. B. Schroeder, E. Esarey, G. Fubiani, D. Auerbach, B. Marcellis *et al.*, *Phys. Rev. Lett.* **91**, 074802 (2003).
- ²⁴W. P. Leemans, J. van Tilborg, J. Faure, C. G. R. Geddes, Cs. Tóth, C. B. Schroeder, E. Esarey, G. Fubiani, and G. Dugan, *Phys. Plasmas* **11**, 2899 (2004).
- ²⁵X. Y. Peng, C. Li, M. Chen, T. Toncian, R. Jung, O. Willi, Y. T. Li, W. M. Wang, S. J. Wang, F. Liu, A. Pukhov, Z. M. Sheng, and J. Zhang, *Appl. Phys. Lett.* **94**, 101502 (2009).
- ²⁶Z. Jiang and X. C. Zhang, *Appl. Phys. Lett.* **72**, 1945 (1998).
- ²⁷Q. Wu, M. Litz, and X. C. Zhang, *Appl. Phys. Lett.* **68**, 2924 (1996).
- ²⁸A. Nahata, A. S. Weling, and T. F. Heinz, *Appl. Phys. Lett.* **69**, 2321 (1996).
- ²⁹J. Fletcher, *Opt. Express* **10**, 1425 (2002).
- ³⁰X. Y. Peng, O. Willi, M. Chen, and A. Pukhov, *Opt. Express* **16**, 12342 (2008).
- ³¹N. H. Matlis, G. R. Plateau, J. van Tilborg, and W. P. Leemans, *J. Opt. Soc. Am. B* **28**, 23 (2011).
- ³²C. Li, M. L. Zhou, W. J. Ding, F. Du, F. Liu, Y. T. Li, W. M. Wang, Z. M. Sheng, J. L. Ma, L. M. Chen, X. Lu, Q. L. Dong, Z. H. Wang, Z. Lou, S. C. Shi, Z. Y. Wei, and J. Zhang, *Phys. Rev. E* **84**, 036405 (2011).
- ³³F. Du, C. Li, M. L. Zhou, W. M. Wang, L. N. Su, Y. Zheng, X. L. Ge, Y. T. Li, J. L. Ma, X. L. Xiu, L. Zhang, Z. M. Sheng, L. M. Chen, X. Lu, Q. L. Dong, Z. H. Wang, Z. Y. Wei, and J. Zhang, *Sci. Chin.* **55**, 43 (2012).
- ³⁴F. Amiranoff, *Meas. Sci. Technol.* **12**, 1795 (2001).
- ³⁵J. Zhang, Y. T. Li, Z. M. Sheng, Z. Y. Wei, Q. L. Dong, and X. Lu, *Appl. Phys. B* **80**, 957 (2005).
- ³⁶Y. T. Li, X. H. Yuan, M. H. Xu, Z. Y. Zheng, Z. M. Sheng, M. Chen, Y. Ma, W. X. Liang, Q. Z. Yu, Y. Zhang, F. Liu, Z. H. Wang, Z. Y. Wei, W. Zhao, Z. Jin, and J. Zhang, *Phys. Rev. Lett.* **96**, 165003 (2006).
- ³⁷X. H. Yuan, Y. T. Li, M. H. Xu, Z. Y. Zheng, M. Chen, W. X. Liang, Q. Z. Yu, Y. Zhang, F. Liu, J. Bernhardt, S. J. Wang, Z. H. Wang, Z. Y. Wei, W. Zhao, and J. Zhang, *Phys. Plasmas* **15**, 013106 (2008).
- ³⁸X. H. Yuan, Y. T. Li, M. H. Xu, Z. Y. Zheng, Q. Z. Yu, W. X. Liang, Y. Zhang, F. Liu, J. Bernhardt, S. J. Wang, Z. H. Wang, W. J. Ling, Z. Y. Wei, W. Zhao, and J. Zhang, *Opt. Express* **16**, 81 (2008).
- ³⁹T. Nakamura, T. Nakamura, S. Kato, H. Nagatomo, and K. Mima, *Phys. Rev. Lett.* **93**, 255002 (2004).
- ⁴⁰C. B. Schroeder, E. Esarey, J. van Tilborg, and W. P. Leemans, *Phys. Rev. E* **69**, 016501 (2004).
- ⁴¹R. Fedosejevs, R. Ottmann, R. Sigel, G. Kühnle, S. Szatmari, and F. P. Schäfer, *Phys. Rev. Lett.* **64**, 1250 (1990).